The new frontiers of gravitational microlensing

M. Dominik

University of St Andrews, Centre for Exoplanet Science, SUPA School of Physics & Astronomy, North Haugh, St Andrews, KY16 9SS, United Kingdom
**E-mail: md35@st-andrews.ac.uk*

Albert Einstein referred to gravitational microlensing as a "most curious effect", and while its underlying principles are intriguingly simple, their universality makes a powerful tool for inferring information about a wide range of astronomical bodies. Much has happened since the first observation of a gravitational microlensing event in 1992, and the frontiers have shifted. What we did not dare dreaming about just a few decades ago turned into reality, and we have not reached the end of the journey. New challenges and opportunities lie ahead. Where might we be able to go and how can we get there?

Keywords: General Relativity – gravitational microlensing – extra-solar planets – black holes

1. General Relativity and the bending of light

Probably the most fascinating feature of the gravitational bending of light is that its underlying principles are strikingly simple. Photons follow null geodesics in the space-time whose curvature as expressed by the Riemann tensor $R_{\mu\nu\rho\sigma}$ corresponds to the energy-momentum tensor $T_{\mu\nu}$ of matter, so that

$$R_{\mu\nu} - \frac{1}{2}\, g_{\mu\nu}\, R = \frac{8\pi G}{c^4}\, T_{\mu\nu}\,, \tag{1}$$

where $R_{\mu\nu} = R^{\alpha}{}_{\mu\alpha\nu}$ is the Ricci tensor and $R^{\alpha}{}_{\alpha}$ is the Ricci scalar.[1]

Outside a localised non-rotating uncharged spherically mass distribution, the space-time with metric tensor $g_{\mu\nu}$ can be described by the Schwarzschild metric[2]

$$\mathrm{d}s^2 = g_{\mu\nu}\,\mathrm{d}q^\mu\,\mathrm{d}q^\nu = \left(1-\frac{r_\mathrm{S}}{r}\right) c^2\mathrm{d}t^2 - \frac{\mathrm{d}r^2}{1-\frac{r_\mathrm{S}}{r}} - r^2\left(\mathrm{d}\theta^2 + \sin^2\theta\,\mathrm{d}\varphi^2\right) \tag{2}$$

for spherical space-time coordinates (t, r, θ, φ), with Schwarzschild's gravitational radius

$$r_\mathrm{S} = \frac{2GM}{c^2} \tag{3}$$

being a key physical scale proportional to the total mass M of the gravitating matter.

With the relativistic Hamilton-Jacobi equation,

$$g^{\mu\nu}\,\frac{\partial S}{\partial q^\mu}\,\frac{\partial S}{\partial q^\nu} = 0\,, \tag{4}$$

which just re-expresses the energy-momentum relation, one finds the action as function of the coordinates and the constants of motion,

$$S = -Et + L\varphi + \int \sqrt{\left(1 - \frac{r_\mathrm{S}}{r}\right)^{-2} \frac{E^2}{c^2} - \left(1 - \frac{r_\mathrm{S}}{r}\right)^{-1} \frac{L^2}{r^2}}\, \mathrm{d}r\,, \tag{5}$$

which are the energy E and the angular momentum L.

Straightforwardly, from the fact that the derivative of the action S with respect to the angular momentum L is constant,

$$\frac{\partial S}{\partial L} = \text{const.}\,, \tag{6}$$

one finds a relation between the polar angle φ and the radial coordinate r

$$\varphi - \varphi_0 = -\int \frac{\mathrm{d}u}{\sqrt{r_\mathrm{S}^2/\xi^2 - u^2(1-u)}}\,, \tag{7}$$

where

$$u \equiv \frac{r_\mathrm{S}}{r} \quad \text{and} \quad \xi \equiv c\,\frac{L}{E}\,. \tag{8}$$

In general, the resulting integral does not have an analytic solution, but it can be solved numerically to yield trajectories. It notably diverges for a closest approach of $r_\mathrm{crit} = 1.5\ r_\mathrm{S}$, at which photons oribit in a circle, although such an orbit is not stable. If one gets close to a black hole, one can see all the interesting effects that strong gravity has on light, as recently beautifully shown by the image of the supermassive black hole in the centre of M87, which reveals the event horizon at the Schwarzschild surface.[3]

For light rays that pass at large distances as compared to the Schwarzschild radius, one can expand the action to first order in r_S/r,

$$S = -Et + L\varphi + \int \sqrt{\frac{E^2}{c^2}\left(1 + 2\,\frac{r_\mathrm{S}}{r}\right) - \frac{L^2}{r^2}}\, \mathrm{d}r\,, \tag{9}$$

and for the relation between φ and r, the arising integral has an analytic solution

$$r(\varphi) = \frac{\xi^2/r_\mathrm{S}}{1 + \sqrt{1 + \xi^2/r_\mathrm{S}^2}\,\cos(\varphi - \varphi_0)}\,, \tag{10}$$

which means that photons follow a hyperbolic path, with the semi-major axis equalling the impact parameter ξ of the light ray and the semi-major axis equalling the Schwarzschild radius r_S, i.e. in particular the eccentricity is given by

$$\varepsilon = \sqrt{1 + \xi^2/r_\mathrm{S}^2}\,. \tag{11}$$

From geometry, one finds for the bending angle α the relation

$$\tan\frac{\alpha}{2} = \frac{r_\mathrm{S}}{\xi}\,, \tag{12}$$

which for small angles is equivalent to

$$\alpha = \frac{2\,r_\mathrm{S}}{\xi}\,. \tag{13}$$

In fact, it was already hypothesised by Isaac Newton in 1704 that gravity should bend light and that the deflection should be strongest at the least distance.[4] A further remarkable feature is that the gravitational bending of light is perfectly achromatic.

The gravitational bending angle was famously measured during the Solar eclipse of 29 May 1919 by two British expeditions to Sobral (in Brazil) and the island of Principe, the latter led by the later-knighted Arthur Eddington.[5,6] The relativistic light bending angle was derived by Einstein in 1915 alongside his discussion of the perihelion precession of Mercury,[7] overriding his earlier findings of 1911 that precede the full development of the Theory of General Relativity, where he proposed half of the amount of deflection.[8]

For a gravitating body that can be approximated as spherical, all the physics at distances much larger than the Schwarzschild radius r_S is summarised in the simple equation for the gravitational bending angle, proportional to the mass M of the deflector, and inversely proportional to the impact parameter ξ of the light ray.

2. Angular Einstein radius and gravitational lens equation

The angular Einstein radius

$$\theta_\mathrm{E} = \sqrt{2\, r_\mathrm{S}\, \frac{\pi_\mathrm{LS}}{1\ \mathrm{AU}}} \tag{14}$$

constitutes the single fundamental scale for the bending of light received from a background star ('source') by an intervening massive body of mass M ('lens'). It derives from the Schwarzschild radius r_S and encompasses the relative lens-source parallax

$$\pi_\mathrm{LS} \equiv \pi_\mathrm{L} - \pi_\mathrm{S} = 1\ \mathrm{AU}\, \left(\frac{1}{D_\mathrm{L}} - \frac{1}{D_\mathrm{S}} \right) , \tag{15}$$

where D_L and D_S denote the distances from the observer to the lens and source, respectively. If these are perfectly aligned as seen by the observer, a ring-shaped image results, whose radius is equal to the angular Einstein radius θ_E.

However, the bended light of the source star can only be observed if the light gets around the foreground body, which means that its angular radius $\theta_\mathrm{L} = R_\mathrm{L}/D_\mathrm{L}$ has to be smaller than the angular Einstein radius θ_E. This implies a lower limit to the lens distance,

$$D_\mathrm{L} \geq \frac{c^2}{4GM}\, R_\mathrm{L}^2 = \frac{3c^2}{16\pi G\rho}\, \frac{1}{R_\mathrm{L}} , \tag{16}$$

where ρ denotes the average mass density. For the Sun, this limit evaluates to 550 AU, whereas an observer on Earth is much closer than that. Eddington and colleagues only saw light coming along one path near the edge of the Sun, not passing either side. For all other foreground stars, light rays wont be blocked. For a given mass density ρ, the minimal distance is inversely proportional to the radius

of the deflector R_L, and for a rock of 20 cm diameter, one would find a far more restrictive limit of $D_\mathrm{L} \geq 100$ Mpc.

Given that the bending angles are tiny, the light trajectory can well be approximated by two straight lines with a change of direction in the plane perpendicular to the line of sight at the position of the gravitational lens. With η denoting the separation of the source star from the line passing through observer and lens, one finds the condition

$$\eta = \frac{D_\mathrm{S}}{D_\mathrm{L}}\,\xi - \alpha(\xi)\,(D_\mathrm{S} - D_\mathrm{L})\ , \tag{17}$$

which with the normalisation

$$x = \frac{\xi}{D_\mathrm{L}\,\theta_\mathrm{E}}\,, \quad u = \frac{\eta}{D_\mathrm{S}\,\theta_\mathrm{E}} \tag{18}$$

assumes the rather simple form

$$u = x - \frac{1}{x}\,, \tag{19}$$

known as the gravitational lens equation for a point-like deflector.

For $u \neq 0$ (i.e. lens and source not perfectly aligned), the ring breaks up into two images,

$$x_\pm = \frac{1}{2}\,\left(u \pm \sqrt{u^2+4}\right)\ , \tag{20}$$

one inside and one outside the Einstein circle. While we lose the rotational symmetry, observer, lens, and source define a plane for the light ray, so that seen from the observer towards the sky, the source, the lens, and the apparent images fall onto a straight line.

3. Gravitational microlensing in the Milky Way

Observing gravitational microlensing requires a close angular alignment between two stars. Given that these move across the sky, they give rise to a transient phenomenon in the form of characteristic 'events'. In order to maximise the chances of seeing these, one would like to monitor stellar fields that are dense enough for many stars to be within the field of view of the camera, but not that dense that lots of stars end up unresolved on the same pixel. Moreover, one should choose a direction that ensures that there are lots of intervening stars that could constitute the gravitational lenses. This makes the galactic bulge a promising choice. Let us see in the following what the properties of Milky Way stars imply for the characteristics of gravitational microlensing events.

Given that we have to rely on chance alignments, we cannot select the intervening bodies, but need to take whatever comes, following the mass function of stellar and sub-stellar objects. The large relative number of low-mass stars makes red dwarfs of 0.3 $M_\odot$ the typical prototype of a lens star, whereas just about 10 % are F and G stars. Moreover, a source star in the dense stellar field of the Galactic bulge,

located a bit behind the Galactic centre, is at about $D_\mathrm{S} \sim 8.5$ kpc distance, while a typical lens star can be found at $D_\mathrm{L} \sim 6.5$ kpc distance. Consequently, for an M-dwarf lens star with 0.3 $M_\odot$, the angular Einstein radius becomes

$$\theta_\mathrm{E} \sim 300\ \mu\mathrm{as} \left(\frac{M}{M_\odot}\right)^{1/2}, \tag{21}$$

which is quite small in comparison to the resolution limits of telescopes. This corresponds to a physical size at the lens distance

$$r_\mathrm{E} = D_\mathrm{L}\,\theta_\mathrm{E} \sim 2\ \mathrm{AU} \left(\frac{M}{M_\odot}\right)^{1/2}, \tag{22}$$

which implies that light rays deflected by a star face a good chance to further get close to a planet. With a typical relative lens-source proper motion of $\mu_\mathrm{LS} \sim 15\ \mu\mathrm{as\,d}^{-1}$, we find an event time-scale

$$t_\mathrm{E} \equiv \frac{\theta_\mathrm{E}}{\mu_\mathrm{LS}} \sim 20\ \mathrm{d} \left(\frac{M}{M_\odot}\right)^{1/2} \tag{23}$$

for gravitational microlensing events, i.e. about a month for a 'typical' stellar lens. With the mass density, one finds an event rate of about 10^{-5} events per year per observed star.[9]

As a source star passes by the lens star, its images move around the Einstein circle. While we cannot resolve these usually (yet!),[a] the fact that the gravitational light bending distorts them results in a time-dependent observable total magnification[11,12b]

$$A(u) = \sum_\pm \left|\frac{x_\pm}{u}\frac{\mathrm{d}x_\pm}{\mathrm{d}u}\right| = \frac{u^2+2}{u\sqrt{u^2+4}}, \tag{24}$$

where

$$u(t) = \sqrt{u_0^2 + \left(\frac{t-t_0}{t_\mathrm{E}}\right)^2}. \tag{25}$$

This means that gravitational microlensing events come with a photometric signature, the first of which being reported in 1993,[13] which was the result of a massive data-processing venture, impossible with the computer technology of earlier times.

For separations much smaller than the angular Einstein radius ($u \ll 1$), one finds $A(u) \simeq 1/u$, and the magnification diverges for $u \to 0$, corresponding to a point being mapped to a circle. While both the duration of a photometric microlensing signature and the probability for it to occur are proportional to the angular Einstein radius θ_E, i.e. proportional to the square-root of the lens mass, $\sqrt{M}$, as long as the

[a] In 2017, Dong et al. succeeded in resolving microlensed images for the first time.[10]

[b] The lens equation relates the radial coordinates x and u, while the polar angle is conserved. Therefore, the magnification becomes the product of the tangential distortion $x_\pm/u$ and the radial distortion $\mathrm{d}x_\pm/\mathrm{d}u$.

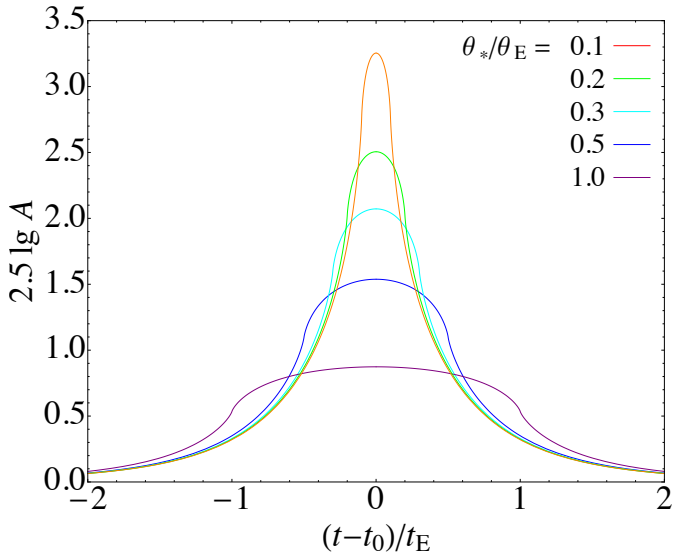

Fig. 1. Brightening in magnitudes $\Delta m = -2.5 \lg A(u)$ as source with angular radius $\theta_\star$ centrally passes behind gravitational lens. The source-lens separation as seen from the observer is $u(t) = |(t - t_0)/t_\mathrm{E}|$, where t_0 marks the epoch of perfect alignment, and $\mu_\mathrm{LS} = \theta_\mathrm{E}/t_\mathrm{E}$ is the lens-source proper motion.

source can be approximated as point-like, the magnification is not limited, larger magnifications are just less probable. For Jupiter-mass lenses ($M \sim 10^{-3}\,M_\odot$), one finds a duration of $\sim$ 1 d, while for Earth-mass lenses ($M \sim 3 \times 10^{-6}\,M_\odot$), this reduces to about $\sim$ 1.5 h.

However, the finite angular radius $\theta_\star$ of the source star imposes the limit

$$A_\mathrm{max} = \sqrt{1 + 4 \left(\frac{\theta_\mathrm{E}}{\theta_\star} \right)^2} \,, \tag{26}$$

which reduces the amplitude of a photometric microlensing signature while increasing the duration, as illustrated in Fig. 1. In fact, the signal duration will become related to the motion of the source star by its diameter

$$2\,t_\star = 2\,\frac{R_\star}{D_\mathrm{S}\,\mu_\mathrm{LS}} \sim 2\ \mathrm{h}\ \frac{R_\star}{R_\odot} \,, \tag{27}$$

as its angular radius $\theta_\star$ is no longer much smaller than the angular Einstein radius θ_E. If one is able to detect deviations as small as 5 %, which implies $\theta_\star/\theta_\mathrm{E} \lesssim 6$, one obtains the limit

$$M \gtrsim 2 \times 10^{-8} \left(\frac{R_\star}{R_\odot} \right)^2 \,, \tag{28}$$

and thereby photometry at that level for stars of Solar radius would mean that foreground objects with masses as small as the Moon can be detected, which comfortably includes planets.

4. Population demographics of planets and smaller bodies

Given the specific sensitivities of the various techniques used to detect planets, the coverage of planet parameter space, as e.g. indicated by planet mass and orbital separation, is patchy and far from uniform (see Fig. 2). Notably, those very regions where we find the Solar System planets are amongst the least explored. Moreover, the vast majority of known planets are within less than 1.5 kpc (or 5,000 light-years) with only gravitational microlensing probing along a single line of sight towards the Galactic centre at larger distances. Given that there are distinct stellar populations, with stars in the galactic disk and bulge having different evolutionary histories and different average properties, we are really not obtaining samples that are characteristic for our galaxy, bust mostly probe the Solar neighbourhood only. How planet demographics look like beyond the Milky Way remains a further open question.

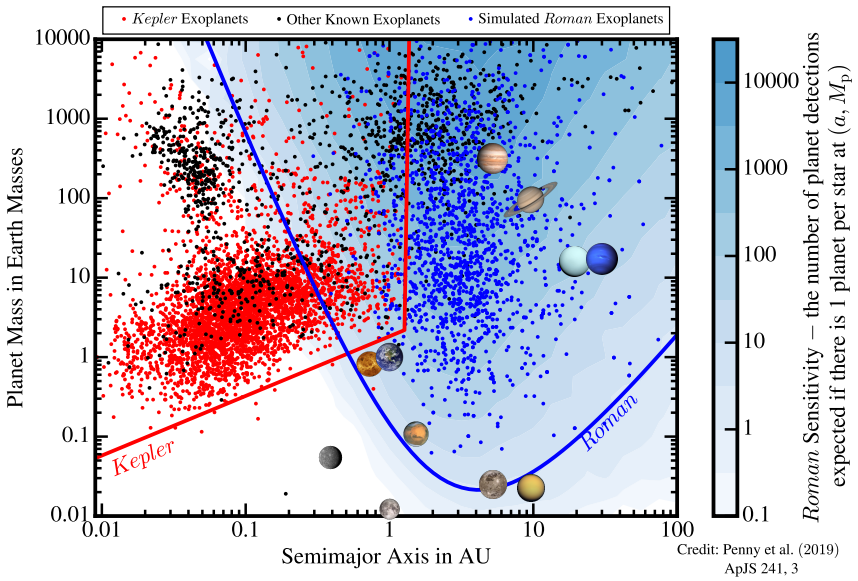

Fig. 2. Demographics of known planets in the Milky Way with regard to their mass and orbital semi-major axis, illustrating the complementarity of planet searches relying on transits or gravitational microlensing. The points in blue are indicative of what a microlensing campaign with the Nancy Grace Roman Space Telescope could deliver (rather than corresponding to actual detections).

The specific characteristics of the phenomena of planetary transits and gravitational microlensing make them complementary for obtaining planet demographics. NASAs Kepler mission has already provided much insight into the planets close to their host stars, whereas a microlensing campaign with the Nancy Grace Roman Space Telescope (formerly called the Wide-Field Infrared Survey Telescope

WFIRST) will explore the regime of planets in wider orbits, and in particular cover planets like those in the Solar System, except for Mercury. With the sensitivity extending down to about Lunar Mass, analogues of the giant moons of Jupiter and Saturn, such as Ganymede and Titan, become detectable.[14]

A "planetary mass function" must *not* be viewed as a low-mass extension of the stellar mass function. Planets do not form as independent objects, but from the circumstellar disk, so that their demographics will naturally depend on the properties of their host star, most prominently its mass and metallicity. Moreover, planet demographics are also characterised by the planetary orbits, so that a differential mass-radius-orbit function

$$\Phi(m_\mathrm{p}, r_\mathrm{p}, a, \varepsilon; M_\star, Z) \tag{29}$$

has at least 6 parameters, namely the planetary mass m_p and radius r_p, the orbital semi-major axis a and eccentricity ε, the stellar mass $M_\star$, and the stellar metallicity Z. Any planet sample corresponds to a weighted average over the underlying specific stellar population.

If we intend to sample a planet population statistic with p parameters, and we want to fit a function to the measured sample abundances sorted into b bins for each parameter, the required sample size for a desired relative precision κ becomes $N = b^p/\kappa^2$.[15] Let us assume that one can obtain an indicative functional behaviour with 5 bins or more and 20 % relative precision. Then a sample of 4000 planets would permit to obtain a function of 3 parameters, e.g. planet mass m_p, planet radius r_p, and stellar mass $M_\star$. If we want to study planets as function of both stellar mass $M_\star$ and metallicity Z, we find ourselves restricted to only one property of the planet. For exploring all major 6 parameters, a sample of about 400 000 planets would be required, 100 times larger than what we have right now. – This is extremely challenging.

Talking about challenges, how far down in mass can one go? As we have seen, the limit arises from the size of the observed source stars, so it is worth thinking about smaller ones. Specifically, white dwarfs are an end-product of stellar evolution, and they are roughly about 100 times smaller than main-sequence stars like the Sun. Therefore, observing those, would push the mass of microlensing searches towards $\sim 1/10\,000$ of the Lunar mass. However, white dwarfs are quite faint, and the signal duration would drop to about a minute, which calls for quite a large telescope to get precision photometry with exposure times of less than 10 seconds. Interestingly, an engineering limit for ground-based telescopes arises from the need to support their weight, which would not be an issue if one assembled a giant telescope in space from smaller parts. Observing short microlensing events on white dwarfs would not only put many satellites and dwarf planets within reach, but would also make asteroids with diameters larger than 200 km detectable, of which the Solar System contains about 40.[16] Light would get around such bodies if they are more distant than about 100 pc, so that one would be able to explore such within planetary systems throughout the Milky Way.

5. Binary lenses and caustics

Let us now consider that the lens is not a single body but instead is composed of N point-like objects of mass M_i, located at position angles $\boldsymbol{\theta}_i = D_\mathrm{L}\,\theta_\mathrm{E}\,\boldsymbol{x}_i$. With $m_i = M_i/M$ denoting the mass fractions, the gravitational lens equation becomes

$$\boldsymbol{u} = \boldsymbol{x} - \sum_{i=1}^{N} m_i \,\frac{\boldsymbol{x}-\boldsymbol{x}_i}{|\boldsymbol{x}-\boldsymbol{x}_i|^2}\,. \tag{30}$$

For such systems, one finds extended lines that describe source positions for which the point-source magnification diverges, or equivalently, the Jacobian determinant of the lens mapping for at least one of the images vanishes. These constitute caustics of the optical system, given by

$$\mathcal{C} = \left\{ \boldsymbol{u}(\boldsymbol{x}_\mathrm{c}) | \det\left(\frac{\partial \boldsymbol{u}}{\partial \boldsymbol{x}}\right)(\boldsymbol{x}_\mathrm{c}) = 0 \right\}\,. \tag{31}$$

A single-mass point lens has a point-like caustic at the position of the lens star, i.e. $u = 0$, which maps to the Einstein circle with an infinite point-source magnification. For binary lenses, this central caustic breaks up into a finite diamond-shaped structure with 4 cusps. More specifically, for any binary gravitational lens, regardless of whether the masses are about equal, or whether we have a star with a small planet, there are 3 different caustic topologies (see Fig. 3), depending on the separation between the two lens objects, and therefore labelled as wide, intermediate, and close.[17–19]

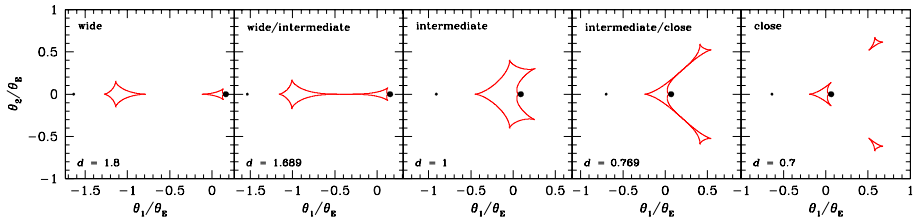

Fig. 3. Topologies of the caustics for a binary gravitational lens. The constituent massive bodies are separated by an angle $d\,\theta_\mathrm{E}$ and the coordinate origin has been chosen as the centre of mass. The positions of the two bodies are indicated by black dots reflecting their respective mass fractions, where the mass ratio is $q = 0.1$.

In turn, the caustic structure of the lens system causes a wide range of possible morphologies of the arising photometric light curve of a binary-lens microlensing event, making its characterisation far from easy.[20]

Shude Mao and Bohdan Pazcyński in 1991 not only suggested that planets could be detected by microlensing, but pointed out that more massive companions should be actually easier to detect.[21] Particularly, gravitational microlensing events provide a yet underexplored opportunity for studying the regime in which planets and brown dwarfs overlap as well as that of close binaries that are otherwise not resolvable.

6. Inferring source properties

Caustics are also useful for scanning the brightness profile of the source, given that there is substantial differential magnification across the stellar disk.

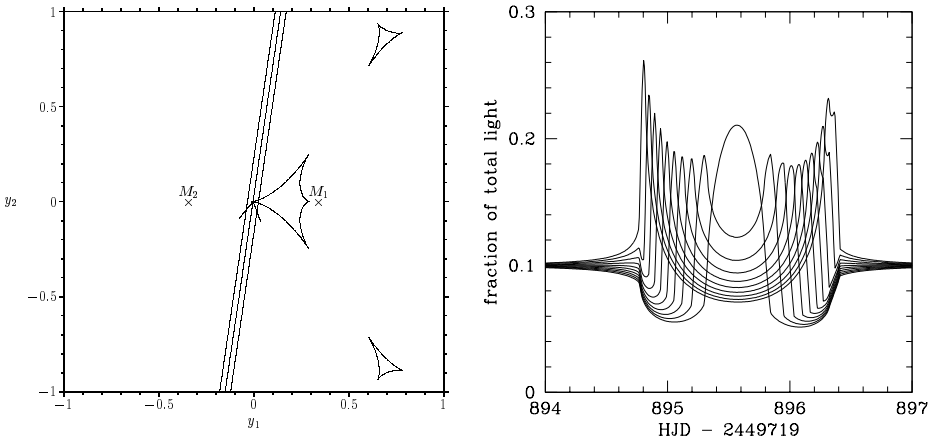

Fig. 4. Differential magnification across the face of the source star in event MACHO 97-BLG-28 as it sweeps over the caustic. The right-hand panel shows the fraction of light contributed by each of the 10 equal-area ring slices as function of time.

For the event MACHO 97-BLG-28, Fig. 4 illustrates how much of the total light comes from each of 10 equal-area ring slices, and one sees how in sequence they take their turn as the star sweeps over the caustic.[22]

A proper motion of 15 $\mu\mathrm{as\,d}^{-1}$ and a 3 min sampling translates into an effective resolution of 30 nas. With stars getting fainter and redder towards the edge, one can also use parametric functions of limb-darkening laws, where for each such profile function one finds a universal fold-caustic magnification function (see Fig. 5).[23–25]

If the observed source star is a binary with a near edge-on orientation towards the observer, it could constitute an eclipsing or a self-lensing binary, depending on how the angular radius of the foreground components θ_L compares to the angular Einstein radius θ_E. Light will be blocked for $\theta_\mathrm{L} \gg \theta_\mathrm{E}$, whereas brightening by gravitational microlensing requires $\theta_\mathrm{L} \ll \theta_\mathrm{E}$. The latter will only occur if one of the objects is a compact stellar remnant,[26–28] and the first such system involving a white dwarf has been reported in 2014.[29] In that case, one sees lensing as the white dwarf passes in front of companion star, but an eclipse as the companion star gets in front of the white dwarf. A Zooniverse citizen science project hunting for black holes as binary self-lensing constituents in the data of the SuperWASP transit search got underway recently.[c]

[c] `https://www.zooniverse.org/projects/hughdickinson/superwasp-black-hole-hunters`

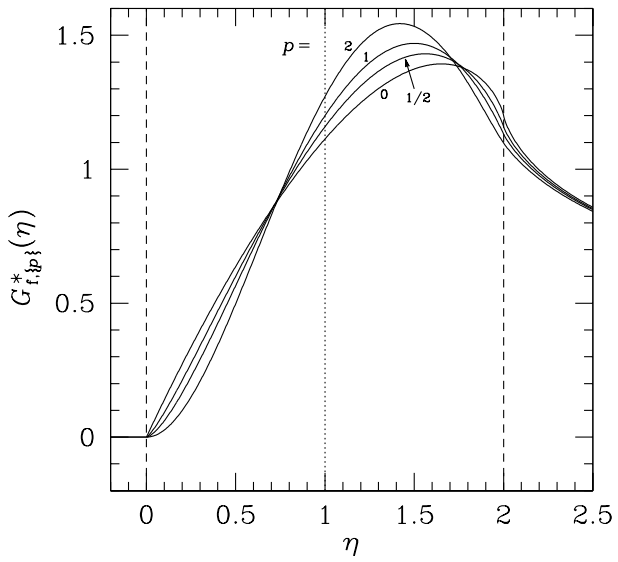

Fig. 5. Universal fold-caustic magnification function $G_{\mathrm{f},\{p\}}(\eta)$ for power-law source brightness profiles $I = \overline{I}(1+p/2)\,(1-\rho^2)^{p/2}$, corresponding to uniform brightness ($p = 0$), as well as square-root ($p = 1/2$), linear ($p = 1$), or quadratic ($p = 2$) limb darkening.

7. Astrometric microlensing, mass measurement, and black holes

The motion of the unresolved images not only alters the observed amount of light, but also displaces its centroid, which constitutes an astrometric signature of gravitational microlensing events, given by

$$\boldsymbol{\delta}(\boldsymbol{u}) = \frac{\boldsymbol{u}}{u^2+2}\,\theta_{\mathrm{E}} \tag{32}$$

and illustrated in Fig. 6.[30–33] In contrast to the photometric signature, it is proportional to the angular Einstein radius θ_{E}, and therefore in principle permits a direct measurement of this characteristic quantity. It is also a vector function, pointing away from the lens star.

If the separation gets large, the image centroid shift drops off far more slowly than the magnification, with $1/u$ rather than its 4^{th} power. Therefore, astrometric microlensing signals remain observable for large lens-source separations for which there is no significant magnification. For small lens-source separations, the image centroid shift becomes proportional to u, $\delta(u) \simeq (u/2)\,\theta_{\mathrm{E}}$, and therefore approaches zero as $u \to 0$, while the magnification tends to infinity. Given that the centroid shift approaches zero for both large and small separations, there must be a maximum, and in fact for an angular separation of $\sqrt{2}\,\theta_{\mathrm{E}}$, a maximal centroid shift of $(\sqrt{2}/4)\,\theta_{\mathrm{E}}$, approximately $0.354\ \theta_{\mathrm{E}}$, occurs.

If one looks at the components of the centroid shift, parallel and perpendicular to the motion of the source star relative to the lens star, one finds that the light

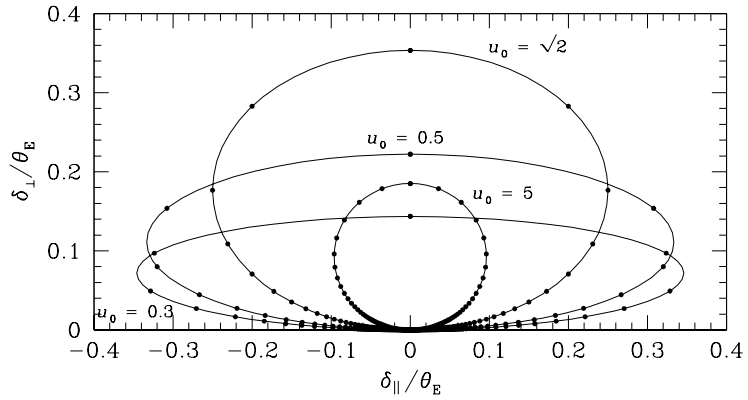

Fig. 6. Microlensing centroid-shift ellipse for various u_0,[33] reflecting that the maximal shift of $(\sqrt{2}/4)\,\theta_\mathrm{E}$ is encountered for $u = \sqrt{2}$. The dots are spaced at equal time intervals of $t_\mathrm{E} = \theta_\mathrm{E}/\mu_\mathrm{LS}$.

centroid traces an ellipse. For large u_0, the ellipse approaches a circle, while for small u_0, it approaches a straight line in parallel direction.

Just about a century after Eddington, the gravitational bending of light was measured for another star: the white dwarf Stein 2051 B,[34] which is in a binary system and the 6th nearest white dwarf known, which means that it is quite bright. From Gaia data, it was predicted that it would approach a more distant star, passing as close as $0.1''$. Positional measurements were made with HST for several epochs, but the much fainter background star could only be resolved for separations larger than about $0.5''$. Nevertheless, the shift in position was clearly seen and delivered an angular Einstein radius $\theta_\mathrm{E} \sim 30$ mas, which then together with the measured parallax provided a measurement of the mass of WD Stein 2051 B, given that

$$M = \frac{c^2}{4G}\,(1\ \mathrm{AU})\,\frac{\theta_\mathrm{E}^2}{\pi_\mathrm{LS}} = \frac{c^2}{4G}\,(1\ \mathrm{AU})\,\frac{\theta_\mathrm{E}}{\pi_\mathrm{E}}\,, \tag{33}$$

where $\pi_E \equiv \pi_\mathrm{LS}/\theta_\mathrm{E}$. In comparison, with the closest angular separation being three times the angular Einstein radius θ_E, the photometric brightening was never substantial. While Eddington measured a deflection by $\sim 2''$, the maximal deflection observed in this case was ~ 2 mas, 1000 times smaller.

As recently explicitly demonstrated by Sahu et al. using HST observations,[35] astrometric microlensing observations can also be used to measure masses of isolated black holes. With the black hole constituting the dark lens, one cannot measure the lens parallax π_L directly, but needs to rely on the source-lens trajectory

$$\boldsymbol{u}(t) = \boldsymbol{u}_0 - (t - t_0)\,\frac{\boldsymbol{\mu}_\mathrm{LS}}{\theta_\mathrm{E}} + \pi_\mathrm{E}\,\boldsymbol{\gamma}(t)\,, \tag{34}$$

for inferring the microlensing parallax parameter π_E from the photometric data, with $\boldsymbol{r}_\oplus(t) = (1\ \mathrm{AU})\,\boldsymbol{\gamma}(t)$ being the projection of the Earth's orbit perpendicular to the line of sight to the observed star. This becomes feasible given that the relatively

large mass of the black hole implies a rather long event time-scale $t_{\rm E}$, so that the observed photometric light curve becomes asymmetric due to a shift in the relative lens-source position caused by the Earth orbiting the Sun. With $\theta_{\rm E}$ then measured from the astrometric signature, one directly finds the mass with Eq. (33).

Moreover, if one can obtain the source distance $D_{\rm S}$ and proper motion $\boldsymbol{\mu}_{\rm S}$, e.g. using Gaia data, one finds the lens distance $D_{\rm S}$ and proper motion $\boldsymbol{\mu}_{\rm L}$ as well. Thereby not only the mass function, but also spatial distribution and kinematics of Black Holes in the Milky Way (except for the radial velocity), could be extracted from a suitable sample of microlensing events.

8. Outlook

Despite the fact that it was the gravitational bending of light near the edge of the Sun that made Albert Einstein and his Theory of General Relativity world-famous, he concluded in 1936 that "here is no great chance of observing this phenomenon" for any other star.[11] However, 50 years of advance in technology made it possible to materialise on a tiny chance of one in a million, and eventually to detect new worlds with masses similar to that of the Earth.

While one cannot get around fundamental limitations, and I discussed several of these, overcoming technical limitations is pretty much a matter of time rather than a matter of principle. Albert Einstein apparently could not foresee what 50 years of technological advance will bring, so I will not even try.

I have shown a few examples rather than giving you a comprehensive discussion, and I would be surprised if there were no further new ideas emerging on how to apply the gravitational bending of light for providing insight on astronomical bodies and phenomena. The "most curious" effect, as Einstein called it, will continue to provide a valuable tool.

References

1. A. Einstein, Die Feldgleichungen der Gravitation, *Sitzungsberichte der Königlich Preußischen Akademie der Wissenschaften* **1915**, 844 (January 1915).
2. K. Schwarzschild, Über das Gravitationsfeld eines Massenpunktes nach der Einsteinschen Theorie, *Sitzungsberichte der Königlich Preußischen Akademie der Wissenschaften* **1916**, 189 (January 1916).
3. Event Horizon Telescope Collaboration *et al.*, First M87 Event Horizon Telescope Results. I. The Shadow of the Supermassive Black Hole, *Astrophys. J. Lett.* **875**, p. L1 (April 2019).
4. I. Newton, *Opticks: or, A treatise of the reflections, refractions, inflexions and colours of light* (Printed for Sam. Smith, and Benj. Walford, Printers to the Royal Society, London, 1704).
5. F. W. Dyson, A. S. Eddington and C. Davidson, A Determination of the Deflection of Light by the Sun's Gravitational Field, from Observations Made at the Total Eclipse of May 29, 1919, *Philosophical Transactions of the Royal Society of London Series A* **220**, 291 (January 1920).

6. R. Ellis, P. G. Ferreira, R. Massey and G. Weszkalnys, 90 years on - the 1919 eclipse expedition at Príncipe, *Astronomy and Geophysics* **50**, 4.12 (August 2009).
7. A. Einstein, Erklärung der Perihelbewegung des Merkur aus der allgemeinen Relativitätstheorie, *Sitzungsberichte der Königlich Preußischen Akademie der Wissenschaften* **1915**, 831 (January 1915).
8. A. Einstein, Über den Einfluß der Schwerkraft auf die Ausbreitung des Lichtes, *Annalen der Physik* **340**, 898 (January 1911).
9. M. Kiraga and B. Paczynski, Gravitational microlensing of the Galactic bulge stars, *Astrophys. J. Lett.* **430**, L101 (August 1994).
10. S. Dong and others., First Resolution of Microlensed Images, *Astrophys. J.* **871**, p. 70 (January 2019).
11. A. Einstein, Lens-Like Action of a Star by the Deviation of Light in the Gravitational Field, *Science* **84**, 506 (December 1936).
12. B. Paczynski, Gravitational Microlensing by the Galactic Halo, *Astrophys. J.* **304**, p. 1 (May 1986).
13. C. Alcock *et al.*, Possible gravitational microlensing of a star in the Large Magellanic Cloud, *Nature* **365**, 621 (October 1993).
14. M. T. Penny, B. S. Gaudi, E. Kerins, N. J. Rattenbury, S. Mao, A. C. Robin and S. Calchi Novati, Predictions of the WFIRST Microlensing Survey. I. Bound Planet Detection Rates, *Astrophys. J. Suppl.* **241**, p. 3 (March 2019).
15. M. Dominik, Planetary mass function and planetary systems, *Mon. Not. R. Astron. Soc.* **411**, 2 (February 2011).
16. Ž. Ivezić *et al.*, Solar System Objects Observed in the Sloan Digital Sky Survey Commissioning Data, *Astron. J.* **122**, 2749 (November 2001).
17. P. Schneider and A. Weiß, The two-point-mass lens – Detailed investigation of a special asymmetric gravitational lens, *Astron. Astrophys.* **164**, 237 (August 1986).
18. H. Erdl and P. Schneider, Classification of the multiple deflection two point-mass gravitational lens models and application of catastrophe theory in lensing, *Astron. Astrophys.* **268**, 453 (February 1993).
19. M. Dominik, The binary gravitational lens and its extreme cases, *Astron. Astrophys.* **349**, 108 (September 1999).
20. C. Liebig, G. D'Ago, V. Bozza and M. Dominik, The complete catalogue of light curves in equal-mass binary microlensing, *Mon. Not. R. Astron. Soc.* **450**, 1565 (June 2015).
21. S. Mao and B. Paczynski, Gravitational Microlensing by Double Stars and Planetary Systems, *Astrophys. J. Lett.* **374**, p. L37 (June 1991).
22. M. D. Albrow *et al.*, Limb Darkening of a K Giant in the Galactic Bulge: PLANET Photometry of MACHO 97-BLG-28, *Astrophys. J.* **522**, 1011 (September 1999).
23. P. Schneider and R. V. Wagoner, Amplification and Polarization of Supernovae by Gravitational Lensing, *Astrophys. J.* **314**, p. 154 (March 1987).
24. P. Schneider and A. Weiss, A gravitational lens origin for AGN-variability ? Consequences of micro- lensing., *Astron. Astrophys.* **171**, 49 (January 1987).
25. M. Dominik, Theory and practice of microlensing light curves around fold singularities, *Mon. Not. R. Astron. Soc.* **353**, 69 (September 2004).
26. C. Leibovitz and D. P. Hube, On the Detection of Black Holes, *Astron. Astrophys.* **15**, p. 251 (November 1971).
27. S. Rahvar, A. Mehrabi and M. Dominik, Compact object detection in self-lensing binary systems with a main-sequence star, *Mon. Not. R. Astron. Soc.* **410**, 912 (January 2011).
28. G. Wiktorowicz, M. Middleton, N. Khan, A. Ingram, P. Gandhi and H. Dickinson,

Predicting the self-lensing population in optical surveys, *Mon. Not. R. Astron. Soc.* **507**, 374 (October 2021).
29. E. Kruse and E. Agol, KOI-3278: A Self-Lensing Binary Star System, *Science* **344**, 275 (April 2014).
30. M. Miyamoto and Y. Yoshii, Astrometry for Determining the MACHO Mass and Trajectory, *Astron. J.* **110**, p. 1427 (September 1995).
31. E. Høg, I. D. Novikov and A. G. Polnarev, MACHO photometry and astrometry., *Astron. Astrophys.* **294**, 287 (February 1995).
32. M. A. Walker, Microlensed Image Motions, *Astrophys. J.* **453**, p. 37 (November 1995).
33. M. Dominik and K. C. Sahu, Astrometric Microlensing of Stars, *Astrophys. J.* **534**, 213 (May 2000).
34. K. C. Sahu *et al.*, Relativistic deflection of background starlight measures the mass of a nearby white dwarf star, *Science* **356**, 1046 (June 2017).
35. K. C. Sahu *et al.*, An Isolated Stellar-Mass Black Hole Detected Through Astrometric Microlensing, arXiv:2201.13296 (January, 2022).